

Deep Dimension Reduction for Supervised Representation Learning

Jian Huang* Yuling Jiao† Xu Liao‡ Jin Liu § Zhou Yu ¶

June 11, 2020

Abstract

The success of deep supervised learning depends on its automatic data representation abilities. Among all the characteristics of an ideal representation for high-dimensional complex data, information preservation, low dimensionality and disentanglement are the most essential ones. In this work, we propose a deep dimension reduction (DDR) approach to achieving a good data representation with these characteristics for supervised learning. At the population level, we formulate the ideal representation learning task as finding a nonlinear dimension reduction map that minimizes the sum of losses characterizing conditional independence and disentanglement. We estimate the target map at the sample level nonparametrically with deep neural networks. We derive a bound on the excess risk of the deep nonparametric estimator. The proposed method is validated via comprehensive numerical experiments and real data analysis in the context of regression and classification.

1 Introduction

Over the past decade, deep learning has achieved remarkable successes in many fields such as computer vision and natural language processing [29, 19, 30]. A key factor for these successes is its automatic data representation capabilities [9]. Among all the characteristics of an ideal representation for high-dimensional complex data, information preservation, low dimensionality and disentanglement are the most essential ones [1]. Information preservation requires that the learned features should be sufficient statistics for estimation and prediction. This can be quantified based on the concept of conditional independence. Low dimensionality

*Department of Statistics and Actuarial Science, University of Iowa, Iowa City, Iowa 52246, USA. jian-huang@uiowa.edu

†School of Mathematics and Statistics, and Hubei Key Laboratory of Computational Science, Wuhan University, Wuhan 430072, P.R. China. (yulingjiaomath@whu.edu.cn)

‡Center of Quantitative Medicine Duke-NUS Medical School, Singapore. liaoxu@u.duke.nus.edu

§Center of Quantitative Medicine Duke-NUS Medical School, Singapore, jin.liu@duke-nus.edu.sg

¶School of Statistics, East China Normal University, Shanghai, 200241, China. zyu@stat.ecnu.edu.cn

means that we should use as few features as possible to represent the underlying structure of the data, and the number of features should be fewer than the ambient dimension. The learned features in the representation can often be interpreted as corresponding to the hidden causes of the observed data, thus disentanglement is an important property to better separate causes from one to another [18]. A representation with these key characteristics can make the model more interpretable and further facilitates the subsequent supervised learning tasks.

It is widely believed that deep neural networks trained in supervised learning learn effective data representation automatically. For example, in classification, the last layer of the deep neural network is a linear classifier and the preceding layers serve as a feature extractor to this classifier. However, there are no explicit formal guiding principles for finding an effective feature representation in the context of supervised deep learning. Indeed, optimizing the standard cross-entropy and least square loss functions for supervised learning (classification and regression) do not guarantee that the learned representations have any desired characteristics. Thus, the standard training procedure does not provide any insights on the black box nature of deep neural networks in terms of feature representation [2].

In this paper, we study the problem of how an ideal representation can be achieved based on the conditional independence principle. We propose a deep dimension reduction (DDR) approach for supervised representation learning. With DDR, we seek a nonlinear dimension reduction map (DRM) from the high-dimensional input space to a lower-dimensional feature space such that the data and its label/response are conditionally independent given the value of the DRM. In the mean time, we regularize the DRM by pushing forward its distribution to the standard Gaussian using the optimal transport method [10, 38, 57]. Therefore, the proposed DDR is guaranteed to have the three desired characteristics of an ideal data representation described above. To quantify the measure for conditional independence, we use the distance covariance [51] that can be estimated easily with samples. Moreover, we match the distribution of the DRM with the standard Gaussian based on minimizing the f -divergence such as the KL and JS divergences. Our main contributions are as follows:

- At the population level, we formulate the ideal representation learning task as that of finding a nonlinear DRM minimizing a loss that characterizes both information preservation and disentanglement.
- We estimate the target DRM at the sample level nonparametrically with deep neural networks and derive a upper bound for the excess risk.
- We validate the proposed DDR via comprehensive numerical experiments and real data analysis in the context of regression and classification. We use the learned features based on DDR as inputs for linear regression and k -nearest neighbor classification. The resulting prediction accuracies are better than or comparable with those based on linear dimension reduction methods for regression and deep learning models for classification. The PyTorch code for DDR is available at <https://github.com/Liao-Xu/DDR>.

1.1 Related works

Supervised dimension reduction: The seminal paper [34] proposed the sufficient dimension reduction via a sliced inverse regression, where the aim is to find a minimum subspace [11] such that the orthogonal projection of the data on to which preserves the dependency of the response on the predictors. There is an extensive literature on sufficient dimension reduction via a linear map [35, 11, 33], see also the review paper [12] and monograph [32] and the references therein. Alternative approaches have been developed to estimate the central space (or its subspace) based on nonparametric estimation of conditional independence [59, 14, 15, 48, 56]. The above mentioned methods focus on linear dimension reduction (LDR). However, LDR may not be effective for high-dimensional complex data such as images and natural languages due to the high nonlinearity of the underlying features.

Representation learning: [53, 46, 43] proposed to study the internal mechanism of supervised deep learning from the perspective of information theory, where they showed that training the deep neural network that optimizes the information bottleneck [52] is a trade-off between the representation and prediction at each layer. To make the information bottleneck idea more practical, deep variational approximation of information bottleneck (VIB) is considered in [3]. Numerical experiments suggest that the learned representations obtained via VIB are favored by the subsequent supervised learning task and robust to adversarial inputs. Information theoretic objectives describing conditional independence such as mutual information are utilized as loss functions to train a representation-learning function i.e. an encoder in the unsupervised setting [21, 40, 55, 36, 47]. Unsupervised models such as VAEs [27] and its variants [25, 20, 54, 37] also learn a representation via its encoder as a by-product.

2 Setup, background and theory

2.1 Setup

Suppose we have a sample of n data-response/lable observations $\{(X_i, Y_i) \subseteq \mathbb{R}^d \times \mathbb{R}^1\}_{i=1}^n$ that are i.i.d. copies of (X, Y) with an unknown law $\mu_{X,Y}$. In many applications, high-dimensional complex data X such as images, texts and natural languages, tend to have low-dimensional representations [9]. Mathematically, we model this phenomenon via assuming the existence of a nonlinear DRM $f^* : \mathbb{R}^d \rightarrow \mathbb{R}^{d^*}$ with $d^* \ll d$ such that the information of X can be completely encoded by f^* in the sense

$$X \perp\!\!\!\perp Y | f^*(X). \tag{1}$$

That is, Y and X are conditionally independent given $f^*(X)$. The representation $f^*(X)$ has much lower dimensionality than X and captures all the information about the statistical dependence of Y on X . We also would like to have the disentanglement property for the

DRM. This can be achieved by transforming the distribution of $f^*(X)$ to standard Gaussian. To this end, we first recall a result in optimal transport theory [10, 38, 57].

Lemma 2.1. Let μ be a probability measures on \mathbb{R}^{d^*} with second order moment and absolutely continuous with respect to the the Gaussian measure γ_{d^*} . Then it admits a unique optimal transportation map $\mathcal{T}^* : \mathbb{R}^{d^*} \rightarrow \mathbb{R}^{d^*}$ such that $\mathcal{T}^*_{\#}\mu = \gamma_{d^*} = \mathcal{N}(\mathbf{0}, \mathbf{I}_{d^*})$. Moreover, \mathcal{T}^* is injective μ -a.e.

Thanks to Lemma 2.1, the map \mathcal{T}^* in Lemma 2.1 transforming the distribution of $f^*(X)$ satisfying (1) to the standard normal distribution. Specifically, define

$$R^* = \mathcal{T}^* \circ f^* : \mathbb{R}^d \rightarrow \mathbb{R}^{d^*}.$$

Then we also have

$$X \perp\!\!\!\perp Y | R^*(X), \quad R^*(X) \sim \mathcal{N}(\mathbf{0}, \mathbf{I}_{d^*}), \quad (2)$$

i.e., R^* is a nonlinear DRM that preserves disentanglement. Note that $f^*(x)$ in (1) is not identifiable. As any injective measurable transformation of $f^*(x)$ also satisfies conditional independence relation (1). However, the sufficient predictor $R^*(X)$ defined in (2) with normality constraint is identifiable up to orthogonal transformations. Then our focus in the next is to find such normally distributed $R(X)$ satisfying conditional independence relation (2).

2.2 Background on distance covariance and f -divergence

Next we recall some results on distance covariance/coorelation [51], which characterizes the dependence of two random variables and can serve as a metric for measuring the conditional independence in (2).

Let i be the imaginary unit $(-1)^{1/2}$. For any $t \in \mathbb{R}^{d^*}$, $s \in \mathbb{R}$, define $\psi_Z(t) = \mathbb{E}[\exp^{it^T Z}]$, $\psi_Y(s) = \mathbb{E}[\exp^{isY}]$, and $\psi_{Z,Y}(t, s) = \mathbb{E}[\exp^{i(t^T Z + sY)}]$ be the characteristic functions of random variables Z, Y , and the pair (Z, Y) , respectively. The squared distance covariance $\mathcal{V}^2(Z, Y)$ is defined as

$$\mathcal{V}^2(Z, Y) = \int_{\mathbb{R}^{d^*+1}} \frac{|\psi_{Z,Y}(t, s) - \psi_Z(t)\psi_Y(s)|^2}{c_* \pi \|t\|^{d^*+1} s^2} dt ds,$$

where $c_* = \frac{\pi^{(d^*+1)/2}}{\Gamma((d^*+1)/2)}$. Let $\mathcal{V}^2(Z) = \mathcal{V}^2(Z, Z)$ and $\mathcal{V}^2(Y) = \mathcal{V}^2(Y, Y)$ be the squared distance variances of Z and Y , respectively. Then the squared distance correlation $\rho^2(Z, Y)$ is defined as

$$\rho^2(Z, Y) = \begin{cases} \frac{\mathcal{V}^2(Z, Y)}{\sqrt{\mathcal{V}^2(Z)\mathcal{V}^2(Y)}} & \text{if } \mathcal{V}^2(Z)\mathcal{V}^2(Y) > 0 \\ 0 & \text{if } \mathcal{V}^2(Z)\mathcal{V}^2(Y) = 0 \end{cases}.$$

An appealing property of distance covariance/correlation is that they characterize the independence, i.e., $Z \perp\!\!\!\perp Y$ is equivalent to $\mathcal{V}(Z, Y) = \rho(Z, Y) = 0$.

Given n i.i.d copies of (Z, Y) , say $\{Z_i, Y_i\}_{i=1}^n$, denote \mathbf{Z} and \mathbf{Y} as the distance matrices with entries

$$\mathbf{Z}_{i,j} = \|Z_i - Z_j\| \quad \text{and} \quad \mathbf{Y}_{i,j} = |Y_i - Y_j|,$$

respectively, $i, j = 1, \dots, n$. [50] proposed an unbiased estimator of the distance covariance $\mathcal{V}^2(Z, Y)$ defined as

$$\widehat{\mathcal{V}}_n^2(Z, Y) = \frac{1}{n(n-3)} \sum_{k \neq l, k, l=1}^n [\mathbf{D}_Z]_{k,l} [\mathbf{D}_Y]_{k,l}, \quad (3)$$

where \mathbf{D}_Z and \mathbf{D}_Y are \mathcal{U} centered distance matrices with entries

$$\begin{aligned} [\mathbf{D}_Z]_{k,l} &= \mathbf{Z}_{k,l} - \frac{1}{n-2} \sum_{i=1}^n \mathbf{Z}_{i,l} - \frac{1}{n-2} \sum_{j=1}^n \mathbf{Z}_{k,j} + \frac{1}{(n-1)(n-2)} \sum_{i,j=1}^n \mathbf{Z}_{i,j}, \\ [\mathbf{D}_Y]_{k,l} &= \mathbf{Y}_{k,l} - \frac{1}{n-2} \sum_{i=1}^n \mathbf{Y}_{i,l} - \frac{1}{n-2} \sum_{j=1}^n \mathbf{Y}_{k,j} + \frac{1}{(n-1)(n-2)} \sum_{i,j=1}^n \mathbf{Y}_{i,j}, \end{aligned}$$

respectively. The sample estimator of $\rho^2(Z, Y)$ can be computed via

$$\widehat{\rho}_n^2(Z, Y) = \begin{cases} \frac{\widehat{\mathcal{V}}_n^2(Z, Y)}{\sqrt{\widehat{\mathcal{V}}_n^2(Z) \widehat{\mathcal{V}}_n^2(Y)}} & \text{if } \widehat{\mathcal{V}}_n^2(Z) \widehat{\mathcal{V}}_n^2(Y) > 0 \\ 0 & \text{if } \widehat{\mathcal{V}}_n^2(Z) \widehat{\mathcal{V}}_n^2(Y) = 0 \end{cases}. \quad (4)$$

[23] showed that $\widehat{\mathcal{V}}_n^2(Z, Y)$ in (3) is a U -statistics with the kernel

$$\begin{aligned} h((Z_1, Y_1), (Z_2, Y_2), (Z_3, Y_3), (Z_4, Y_4)) &= \frac{1}{4} \sum_{\substack{1 \leq i, j \leq 4, \\ i \neq j}} \|Z_i - Z_j\| |Y_i - Y_j| \\ &- \frac{1}{4} \sum_{i=1}^4 \left(\sum_{\substack{1 \leq j \leq 4, \\ j \neq i}} \|Z_i - Z_j\| \sum_{\substack{1 \leq j \leq 4, \\ i \neq j}} |Y_i - Y_j| \right) \\ &+ \frac{1}{24} \sum_{\substack{1 \leq i, j \leq 4, \\ i \neq j}} \|Z_i - Z_j\| \sum_{\substack{1 \leq i, j \leq 4, \\ i \neq j}} |Y_i - Y_j| \end{aligned}, \quad (5)$$

where $(Z_i, Y_i), i = 1, \dots, 4$ are i.i.d. copy of (Z, Y) . So we can write

$$\widehat{\mathcal{V}}_n^2(Z, Y) = \frac{1}{C_n^4} \sum_{1 \leq i_1 < i_2 < i_3 < i_4 \leq n} h((Z_{i_1}, Y_{i_1}), \dots, (Z_{i_4}, Y_{i_4})) \quad (6)$$

Let μ_Z and γ be two probability measures on \mathbb{R}^{d^*} . The f -divergence [4] between μ_Z and γ with $\mu_Z \ll \gamma$ is defined as

$$\mathbb{D}_f(\mu_Z \| \gamma) = \int_{\mathbb{R}^{d^*}} f\left(\frac{d\mu_Z}{d\gamma}\right) d\gamma, \quad (7)$$

where $f : \mathbb{R}^+ \rightarrow \mathbb{R}$ is a twice-differentiable convex function satisfying $f(1) = 0$. The KL divergence and JS divergence correspond to $f(t) = t \log t$ and $f(t) = -(t+1) \log \frac{1+t}{2} + t \log t$, respectively. By Jensen's inequality, $\mathbb{D}_f(\mu_Z \| \gamma) = 0$ implies $\mu_Z = \gamma$ almost everywhere.

Denote \mathfrak{F} as the Fenchel conjugate of f [42]. Then the f -divergence admits the following variational formulation [39].

Lemma 2.2.

$$\mathbb{D}_f(\mu_Z \|\gamma) = \max_{D: \mathbb{R}^{d^*} \rightarrow \text{dom}(\mathfrak{F})} \mathbb{E}_{Z \sim \mu_Z} [D(Z)] - \mathbb{E}_{W \sim \gamma} [\mathfrak{F}(D(W))], \quad (8)$$

where the maximum is attained when $D(x) = f'(\frac{d\mu_Z}{d\gamma}(x))$.

2.3 Deep nonparametric estimation of DRM

With the above preparation, we show that at the population level, one can construct a loss function such that the target R^* in (2) is a global minimizer.

Theorem 2.1. Let $\mathcal{R} = \{R \mid \text{measurable map} : \mathbb{R}^d \rightarrow \mathbb{R}^{d^*}, R(X) \sim \gamma_{d^*}, (X, Y) \sim \mu_{X, Y} \text{ and } X \sim \mu_X\}$. For any $R \in \mathcal{R}$, $\lambda > 0$, define

$$\mathcal{L}(R) = \max_{D: \mathbb{R}^{d^*} \rightarrow \text{dom}(\mathfrak{F})} \{\mathbb{E}_{X \sim \mu_X} [D(R(X))] - \mathbb{E}_{W \sim \gamma_{d^*}} [\mathfrak{F}(D(W))]\} - \lambda \mathcal{V}^2(R(X), Y). \quad (9)$$

Then

$$R^* \in \arg \min_{R \in \mathcal{R}} \mathcal{L}(R)$$

provided (2) holds.

According to Theorem 2.1, we can estimate the target R^* from a random sample $\{(X_i, Y_i)\}_{i=1}^n$ nonparametrically with deep neural networks. Let $\mathcal{N}_{\mathcal{D}, \mathcal{W}, \mathcal{S}, \mathcal{B}} \subseteq \mathcal{R}$ be the set of ReLU neural networks R_θ with parameter θ , depth \mathcal{D} , width \mathcal{W} , size \mathcal{S} , and $\|R_\theta\|_\infty \leq \mathcal{B}$. Similarly, denote $\mathcal{M}_{\bar{\mathcal{D}}, \bar{\mathcal{W}}, \bar{\mathcal{S}}, \bar{\mathcal{B}}}$ as the set of ReLU neural networks $D_\phi : \mathbb{R}^{d^*} \rightarrow \mathbb{R}$. Let $\{W_i\}_{i=1}^n$ be n i.i.d random variables drawn from γ_{d^*} . Define,

$$\widehat{R}_\theta \in \arg \min_{R_\theta \in \mathcal{N}_{\mathcal{D}, \mathcal{W}, \mathcal{S}, \mathcal{B}}} \widehat{\mathcal{L}}(R_\theta) = \widehat{D}_f(\mu_{R_\theta(X)} \|\gamma_{d^*}) - \lambda \widehat{\mathcal{V}}_n^2(R_\theta(X), Y), \quad (10)$$

where

$$\widehat{\mathcal{V}}_n^2(R_\theta(X), Y) = \frac{1}{C_n^4} \sum_{1 \leq i_1 < i_2 < i_3 < i_4 \leq n} h((R_\theta(X_{i_1}), Y_{i_1}), \dots, (R_\theta(X_{i_4}), Y_{i_4})), \quad (11)$$

and

$$\widehat{D}_f(\mu_{R_\theta(X)} \|\gamma_{d^*}) = \max_{D_\phi \in \mathcal{M}_{\bar{\mathcal{D}}, \bar{\mathcal{W}}, \bar{\mathcal{S}}, \bar{\mathcal{B}}}} \frac{1}{n} \sum_{i=1}^n [D_\phi(R_\theta(X_i)) - \mathfrak{F}(D_\phi(W_i))]. \quad (12)$$

The second term $-\lambda \widehat{\mathcal{V}}_n^2(R_\theta(X), Y)$ in (10) is an unbiased and consistent estimator of $-\lambda \mathcal{V}^2(R_\theta(X), Y)$, which measures the conditional independence $X \perp\!\!\!\perp Y | R_\theta(X)$. The first term $\widehat{D}_f(\mu_{R_\theta(X)} \|\gamma_{d^*})$ in (10) is the dual form of the f -GAN loss that guarantees the

disentanglement of $R_\theta(X)$. Next we bound the excess risk $\mathcal{L}(\widehat{R}_\theta) - \mathcal{L}(R^*)$ of the deep nonparametric estimator \widehat{R}_θ in (10).

Theorem 2.2. Assume R^* is Lipschitz continuous with Lipschitz constant L_1 and $\text{supp}(\mu_X) \subseteq [-B_1, B_1]^d$. For some finite number of $R \in \mathcal{N}_{\mathcal{D}, \mathcal{W}, \mathcal{S}, \mathcal{B}}$, assume $r(z) = \frac{d\mu_{R(X)}}{d\gamma_{d^*}}(z)$ is Lipschitz continuous with Lipschitz constant L_2 , and $0 < c_1 \leq r(z) \leq c_2$. Denote $B_2 = \max\{|f'(c_1)|, |f'(c_2)|\}$, $B_3 = \max_{|s| \leq 2L_2\sqrt{d^*} \log n + B_2} |\mathfrak{F}(s)|$. Set the network parameters of $\mathcal{N}_{\mathcal{D}, \mathcal{W}, \mathcal{S}, \mathcal{B}}$ and $\mathcal{M}_{\widehat{\mathcal{D}}, \widehat{\mathcal{W}}, \widehat{\mathcal{S}}, \widehat{\mathcal{B}}}$ such that depth $\mathcal{D} = 9 \log n + 12$, width $\mathcal{W} = d^* \max\{8d(n^{\frac{d}{2+d}} / \log n)^{\frac{1}{d}} + 4d, 12n^{\frac{d}{2+d}} / \log n + 14\}$, size $\mathcal{S} = d^* n^{\frac{d-2}{d+2}} / \log^4(ddd^*)$, $\mathcal{B} = (2B_3L_1\sqrt{d} + \log n)\sqrt{d^*}$, and depth $\widehat{\mathcal{D}} = 9 \log n + 12$, width $\widehat{\mathcal{W}} = \max\{8d^*(n^{\frac{d^*}{2+d^*}} / \log n)^{\frac{1}{d^*}} + 4d^*, 12n^{\frac{d^*}{2+d^*}} / \log n + 14\}$, size $\widehat{\mathcal{S}} = n^{\frac{d^*-2}{d^*+2}} / (\log^4 ddd^*)$, $\widehat{\mathcal{B}} = 2L_2\sqrt{d^*} \log n + B_2$. Let $\lambda = \mathcal{O}(1)$, then,

$$\mathbb{E}_{\{X_i, Y_i, W_i\}_{i=1}^n} [\mathcal{L}(\widehat{R}_\theta) - \mathcal{L}(R^*)] \leq C((L_1 + L_2)\sqrt{dd^*}n^{-\frac{2}{2+d}} + L_2\sqrt{d^*} \log nn^{-\frac{2}{2+d^*}}),$$

where, C is a constant that depends on B_1, B_2, B_3 but not depend on n, d and d^* .

3 Deep dimension reduction algorithm

Theorem 2.2 implies that the deep nonparametric estimator \widehat{R}_θ in (10) serves as a good estimator of ideal nonlinear dimension reduction map R^* . Then, we train R_θ according to the loss in (10) in two steps iteratively as follows:

- (i) Update the discriminator D_ϕ : Fix θ and calculate the loss for ϕ in (12) and ascending this loss by SGD on ϕ .
- (ii) Update the reducer R_θ : Compute the loss for θ in (10) with the updated ϕ in (i) and descend this loss by SGD on θ .

Lemma 2.2 implies that the training on ϕ in (i) is to get an optimal discriminator D_ϕ to approximate the optimal dual function $D(x) = f'(\frac{d\mu_{R_\theta(X)}}{d\gamma_{d^*}}(x))$. We implement the second step (ii) using the particle methods based on gradient flow in probability measure spaces [17, 16]. The key idea of this particle method is to formulate the optimization problem in step (ii) into a problem of seeking a sequence of nonlinear residual maps, say \mathbb{T} , pushing the samples from a distribution to the target distribution. The residual maps can be estimated via deep density-ratio estimators, see [16] for details. Here, we use this approach to transform $Z_i = R_\theta(X_i), i = 1, \dots, n$ into Gaussian samples (we still denote them as Z_i) directly. Once this is done, we update θ via minimizing the loss $\sum_{i=1}^n \|R_\theta(X_i) - Z_i\|^2/n - \lambda \widehat{\mathcal{V}}_n^2(R_\theta(X), Y)$. We depict the DDR algorithm in a flowchart in Figure 1 and give a detailed description below.

- Deep dimension reduction algorithm
- Input $\{X_i, Y_i\}_{i=1}^n$. Tuning parameters: s, λ, d^* . Sample $\{W_i\}_{i=1}^n \sim \gamma_{d^*}$.

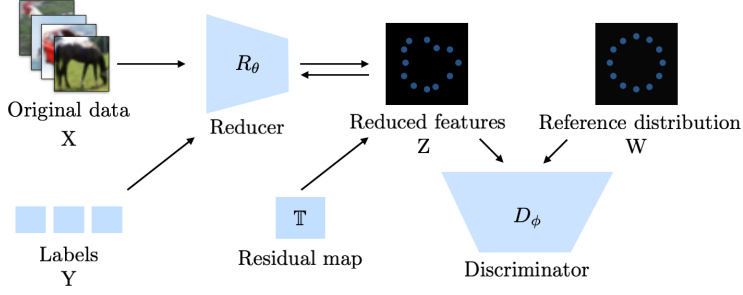


Figure 1: Flow chart for DDR

- **Outer loop for θ**
 - **Inner loop (particle method)**
 - * Let $Z_i = R_\theta(X_i), i = 1, 2, \dots, n$.
 - * Solve $\hat{D}_\phi \in \arg \min_{D_\phi} \sum_{i=1}^n \frac{1}{n} (\log(1 + \exp^{-D_\phi(Z_i)}) + \log(1 + \exp^{D_\phi(W_i)}))$ with SGD.
 - * Define the residual map $\mathbb{T} = \mathbf{I} - s f''(\hat{r}(x)) \nabla \hat{r}(x)$ with $\hat{r}(x) = \exp^{-\hat{D}_\phi(\mathbf{x})}$.
 - * Update the particles $Z_i = \mathbb{T}(Z_i), i = 1, 2, \dots, n$.
 - **End inner loop**
 - Update θ via minimizing $\sum_{i=1}^n \|R_\theta(X_i) - Z_i\|^2/n - \lambda \hat{\mathcal{V}}_n^2(R_\theta(X), Y)$ with SGD.
- **End outer loop**

4 Experiments

We evaluate the proposed DDR using both simulated and real data. Details on the network structures and hyperparameters are included in the appendix. Our experiments were conducted on Nvidia DGX Station workstation using a single Tesla V100 GPU unit. The PyTorch code of DDR is available at <https://github.com/Liao-Xu/DDR>.

4.1 Toy Examples

In this subsection, we evaluate DDR on simulated regression and classification problems.

Regression. We generate 5000 data from the following models:

- Model A: $Y = \frac{X_1}{0.5+(X_2+1.5)^2} + (1 + X_2)^2 + \sigma\epsilon$, where $X \sim N(\mathbf{0}, \mathbf{I}_4)$, $\epsilon \sim N(\mathbf{0}, \mathbf{I}_4)$;
- Model B: $Y = \sin^2(\pi X_1 + 1) + \sigma\epsilon$, where $X \sim \text{Unifrom}([0, 1]^4)$.

R_θ is a 3-layer network with ReLU activation for both Model A and Model B. D_ϕ for both Model A and Model B is a single hidden layer ReLU network. We compare DDR with

two linear dimension reduction methods: sliced inverse regression (SIR) [34] and sliced average variance estimation (SAVE) [44]. We fit a linear model with the learned features and the response variable, and report the prediction error in Table 1. We can see that DDR outperforms SIR and SAVE in terms of prediction error.

Table 1: Averaged prediction errors and their standard errors (based on 5-fold validation).

METHODS	MODEL A			MODEL B		
	$\sigma = 0.1$	$\sigma = 0.4$	$\sigma = 0.8$	$\sigma = 0.1$	$\sigma = 0.2$	$\sigma = 0.3$
DDR	1.101 \pm .193	1.179 \pm .117	1.401 \pm .159	0.149 \pm .050	0.231 \pm .025	0.325 \pm .026
SIR	1.521 \pm .133	1.614 \pm .223	1.704 \pm .095	0.266 \pm .003	0.319 \pm .004	0.391 \pm .010
SAVE	1.521 \pm .134	1.614 \pm .221	1.702 \pm .098	0.266 \pm .003	0.319 \pm .004	0.391 \pm .010

Classification. We visualize the learned features of DDR on three simulated data. We first generated (1) 2-dimensional concentric circles from two classes see Figure 2 (a); (2) 2-dimensional moons data from two classes, see Figure 2 (e); (3) 3-dimensional Gaussian data from six classes, see Figure 2 (i). In all three datasets, we have 5,000 data points for each class. Next, we map these data points into points in \mathbb{R}^{100} by multiplying matrices with entries i.i.d Unifrom([0,1]). We then apply DDR to these 100-dimensional datasets with their labels to learn 2-dimensional features. We use a 10-layer dense convolutional network (DenseNet) [22] as R_θ and adopt a 4-layer network with Leaky ReLU activation as D_ϕ . We display the evolutions of the learned 2-dimensional features by DDR with scatter plots in Figure 2. Clearly, the learned features for different classes in all three examples are disentangled well.

4.2 Real datasets

Regression. We use the benchmark Boston housing dataset <https://www.cs.toronto.edu/~delve/data/boston/bostonDetail.html> and YearPredictionMSD dataset <https://archive.ics.uci.edu/ml/datasets/YearPredictionMSD> to demonstrate the performance of DDR. The Boston housing dataset consists of 506 observations with 13 predictors. The response variable is the median housing price. The YearPredictionMSD dataset has 515,345 observations with 90 predictors. The goal with this dataset is to predict the year of song release. Each dataset was randomly split into five parts for 5-fold validation. We employed a 3-layer network as D_ϕ . A 2-layer network and a 3-layer network were used for R_θ for the Boston housing dataset and the YearPredictionMSD dataset, respectively. The Leaky ReLU activation function was used in all the networks. A linear regression model was adopted to fit the learned representation and the response for each dataset. The mean prediction errors and their standard errors based on DDR, principal component analysis (PCA), sparse principal component analysis (SPCA) and linear regression with original data (LR) are reported in Table 2. We can see that DDR outperforms PCA, SPCA and the linear model

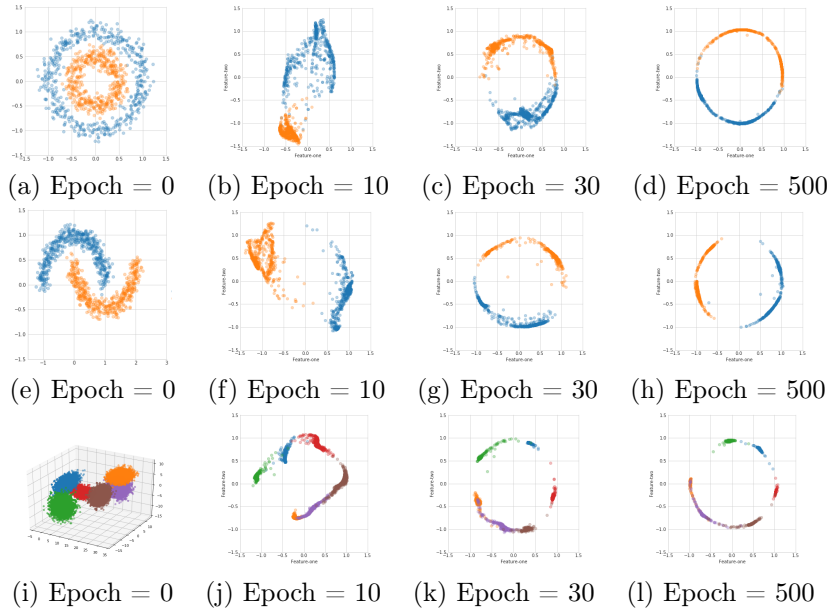


Figure 2: Scatter plots of the evolving learned features. The first, second and third rows demonstrate concentric circles, moons and 3D Gaussian datasets, respectively.

without dimension reduction in terms prediction accuracy for both datasets.

Table 2: Prediction errors for Boston housing dataset and YearPredictionMSD dataset with different d^* (based on 5-fold validation).

METHODS	BOSTON HOUSING				YEARPREDICTIONMSD			
	$d^* = 3$	$d^* = 5$	$d^* = 7$	$d^* = 9$	$d^* = 10$	$d^* = 20$	$d^* = 30$	$d^* = 40$
DDR	4.1 \pm 1.2	4.1 \pm 1.2	4.5 \pm 1.4	5.0 \pm 2.0	8.8 \pm 0.1	9.2 \pm 0.8	9.2 \pm 0.8	8.8 \pm 0.1
SPCA	5.3 \pm 1.5	5.3 \pm 1.8	5.3 \pm 1.8	5.4 \pm 1.8	10.6 \pm 0.1	10.4 \pm 0.1	9.6 \pm 0.1	10.2 \pm 0.1
PCA	5.4 \pm 1.5	5.3 \pm 1.7	5.3 \pm 1.7	5.3 \pm 1.7	10.6 \pm 0.1	10.4 \pm 0.1	10.3 \pm 0.1	10.2 \pm 0.1
LR		5.8 \pm 1.8				9.6 \pm 0.1		

Classification. We use the benchmark datasets MNIST [31], FashionMNIST [60] and CIFAR-10 [28] to evaluate the performance of DDR. The MNIST and FashionMNIST datasets consist of 60k and 10k grayscale, 28×28 -pixel images for training and testing, respectively. The CIFAR-10 contains 50k and 10k 32×32 -pixel colored images for training and testing, respectively. For CIFAR-10, the images of the training set were preprocessed by random crops and horizontal flips. We adopted an architecture modified from the DenseNet networks as R_θ , where R_θ has 20 layers for MNIST and 100 layers for CIFAR10. D_ϕ is a 4-layer network. The architectures and hyperparameters settings were shared across all the methods considered here. We compare DDR with the feature extractor obtained via dropping the cross entropy layer of the DenseNet trained for classification (CN) and distance correlation

autoencoder (dCorAE) [58]. Finally, we use the k -nearest neighbor ($k = 5$) classifier on the learned features from each method. The classification accuracies were reported in Table 3. We can see that the classification accuracies of DDR are comparable with those of CN and dCorAE. We also calculated the estimated distance correlation (DC) using (4) between the learned features and their labels. We plot the DC values in Figure 3, which shows that DDR tends to achieve higher DC values, especially when the data is more complex, e.g., CIFAR-10 here.

Table 3: Classification accuracy for comparison on MNIST, FashionMNIST and CIFAR-10.

d^*	MNIST			FASHIONMNIST			CIFAR-10		
	DDR	dCORAE	CN	DDR	dCORAE	CN	DDR	dCORAE	CN
$d^* = 16$	99.41	99.58	99.39	94.44	94.18	94.21	94.29	94.15	94.21
$d^* = 32$	99.61	99.54	99.45	94.18	93.89	94.41	94.58	94.18	94.92
$d^* = 64$	99.56	99.53	99.49	94.13	94.24	94.38	94.46	94.66	95.09

5 Conclusion

In this work, we propose a deep dimension reduction approach to achieving a good data representation for supervised learning with certain desired characteristics including information preservation, low-dimensionality and disentanglement. We formulate the ideal representation learning task as that of finding a nonlinear dimension reduction map that minimizes the sum of losses characterizing conditional independence and disentanglement. We derive an upper bound on the excess risk of the deep nonparametric estimator. The proposed method is validated via comprehensive numerical experiments and real data analysis in the context of regression and classification. For the future work, it would be interesting to consider other measures of conditional independence and generalize the proposed method to semi-supervised learning problems.

Acknowledgements

The work of Jian Huang is supported in part by the NSF grant DMS-1916199. The work of Y. Jiao is supported in part by the National Science Foundation of China under Grant 11871474 and by the research fund of KLATASDSMOE. The work of J. Liu is supported by Duke-NUS Graduate Medical School WBS: R913-200-098-263 and MOE2016- T2-2-029 from Ministry of Education, Singapore. The work of Z. Yu is supported in part by the National Science Foundation of China under Grant 11971170. This research is supported by the Suppercomputing Center of Wuhan University.

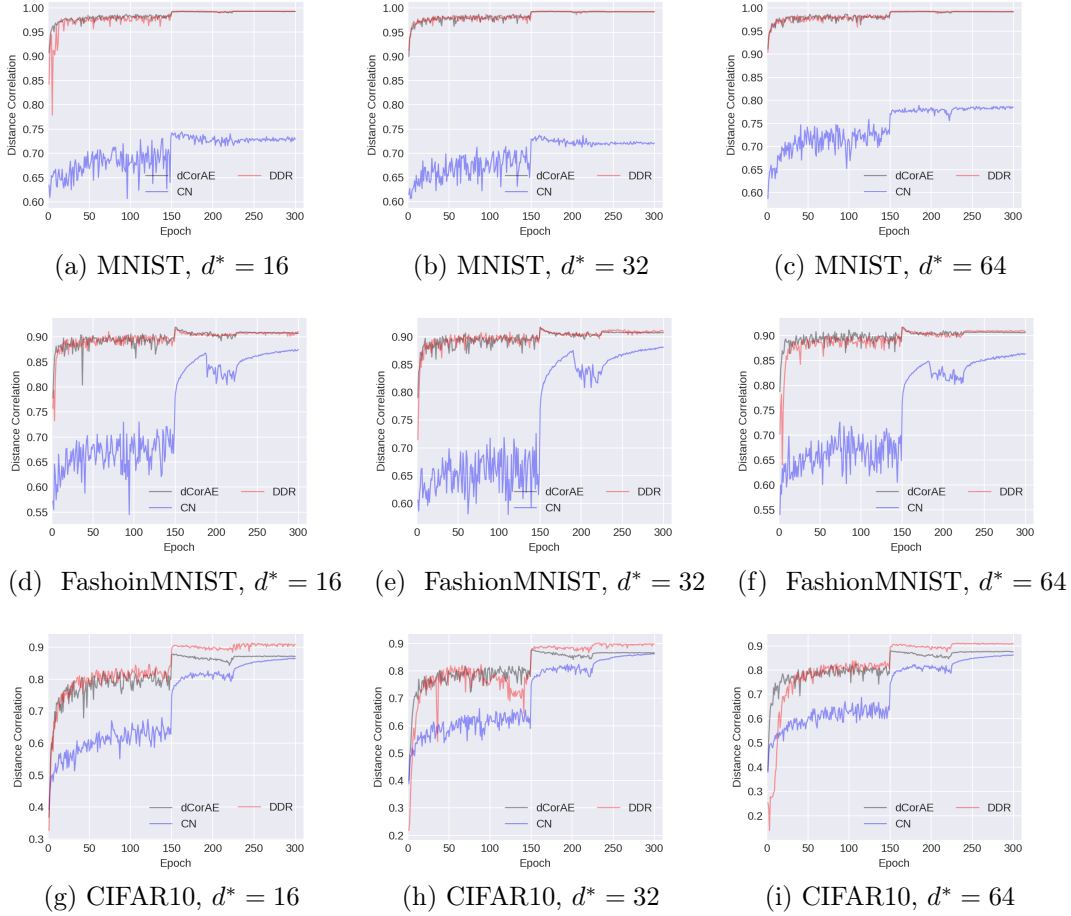


Figure 3: The estimated distance correlations of labels with features from DDR, CN and dCorAE for MNIST, FashionMNIST and CIFAR10.

In the appendix, we give the implementation details on numerical settings, network structures, SGD optimizers, and hyper-parameters in the paper, and detailed proofs of Lemmas 2.1-2.2, Theorems 2.1-2.2.

A Experimental details

A.1 Toy examples

Regression & Classification: For classification toy examples, detailed hyper-parameters for toy example experiments can be found in Table 4. We note that λ is the penalty coefficient, d^* is the dimension of reduced features, M is the mini-batch size in Stochastic Gradient Descent (SGD), T_1 is the number of inner loops to push forward particles Z_i , T_2 is the

number of outer loops to train R_θ , and s is the step size to update particles. As Table 5 shows, a multilayer perceptron (MLP) was utilized for the neural structure D_ϕ . The detailed architecture of 10-layer dense convolutional network (DenseNet) [22, 5] deployed for R_θ is shown in Table 6. For all settings, we adopted Adam [26] optimizer with an initial learning rate of 0.001 and weight decay of 0.0001.

Table 4: Hyper-parameters in DDR on toy examples, where s varies according to epoch.

Task	λ	d^*	M	T_1	T_2	s		
						0-150	151-225	226-500
Regression	1.0	2 or 1	64	1	500	3.0	2.0	1.0
Classification	1.0	2	64	1	500	2.0	1.5	1.0

Table 5: MLP architecture for D_ϕ of toy classification examples and classification tasks on the benchmark datasets.

Layers	Details	Output size
Layer 1	Linear, LeakyReLU	64
Layer 2	Linear, LeakyReLU	128
Layer 3	Linear, LeakyReLU	64
Layer 4	Linear	1

A.2 Real datasets

Regression: In the regression task, hyper-parameters of DDR are demonstrated in Table 7. For neural networks trainings on both datasets, Adam optimizer with an initial learning rate of 0.001 and weight decay of 0.0001 was adopted. DDR models with MLP were employed for the benchmark datasets. The MLP architecture of D_ϕ and R_θ for Boston Housing dataset are shown in Table 8 and Table 9, respectively, while details of R_θ for YearPredictionMSD dataset are shown in Table 8.

Classification:

We set SGD optimizers as Adam for both D_ϕ and R_θ . In details, learning rate of 0.001 and weight decay of 0.0001 are used for D_ϕ in all datasets and for R_θ on MNIST [31]. We customized SGD optimizers with momentum at 0.9, weight decay at 0.0001, and learning rate ρ in Table 11 for FashionMNIST [60] and CIFAR-10 [29], MLP architectures were deployed for D_ϕ on MNIST, FashionMNIST and CIFAR-10, with details that shown in Table 5. The 20-layer DenseNet networks shown in Table 12 were utilized for R_θ on the MNIST dataset,

Table 6: DenseNet architecture for R_θ of toy classification examples.

Layers	Details	Output size
Convolution	3×3 Conv	$24 \times 20 \times 20$
Dense Block 1	$\left[\begin{array}{l} \text{BN, } 1 \times 1 \text{ Conv} \\ \text{BN, } 3 \times 3 \text{ Conv} \end{array} \right] \times 1$	$36 \times 20 \times 20$
Transition Layer 1	BN, ReLU, 2×2 Average Pool, 1×1 Conv	$30 \times 10 \times 10$
Dense Block 2	$\left[\begin{array}{l} \text{BN, } 1 \times 1 \text{ Conv} \\ \text{BN, } 3 \times 3 \text{ Conv} \end{array} \right] \times 1$	$18 \times 10 \times 10$
Transition Layer 2	BN, ReLU, 2×2 Average Pool, 1×1 Conv	$15 \times 5 \times 5$
Dense Block 3	$\left[\begin{array}{l} \text{BN, } 1 \times 1 \text{ Conv} \\ \text{BN, } 3 \times 3 \text{ Conv} \end{array} \right] \times 1$	$27 \times 5 \times 5$
Pooling	BN, ReLU, 5×5 Average Pool, Reshape	27
Fully connected	Linear	2

Table 7: Hyper-parameters in DDR on the regression benchmark datasets.

Dataset	λ	d^*	M	T_1	T_2	s
YearPredictionMSD	1.0	10, 20, 30, 40	64	1	500	1.0
Boston Housing	1.0	3, 5, 7, 9	64	1	500	1.0

Table 8: MLP architectures for D_ϕ and R_θ on the regression benchmark datasets.

Layers	D_ϕ for both datasets		R_θ for YearPredictionMSD	
	Details	Output size	Details	Output size
Layer 1	Linear, LeakyReLU	32	Linear, LeakyReLU	32
Layer 2	Linear, LeakyReLU	8	Linear, LeakyReLU	8
Layer 3	Linear	1	Linear	d^*

Table 9: MLP architecture for R_θ on Boston Housing dataset.

Layers	Details	Output size
Layer 1	Linear, LeakyReLU	8
Layer 2	Linear	1

while the 100-layer DenseNet networks shown in Table 13 and 14 were fitted for R_θ on FashionMNIST and CIFAR-10.

Table 10: Hyper-parameters in DDR on the classification benchmark datasets.

Dataset	λ	d^*	M	T_1	T_2	s
MNIST	1.0	16, 32, 64	64	1	300	0.1
FashionMNIST	1.0	16, 32, 64	64	1	300	1.0
CIFAR-10	1.0	16, 32, 64	64	1	300	1.0

Table 11: Learning rate ρ varies during training.

Epoch	0-150	151-225	226-300
ρ	0.1	0.01	0.001

B Proofs

B.1 Proof of Lemma 2.1

Proof. By assumption μ and γ_{d^*} are both absolutely continuous with the Lebesgue measure. Then the desired result holds since it is a special case of the well known results on the existence of optimal transport [10, 38], see, Theorem 1.28 on page 24 of [41] for detail. \square

B.2 Proof of Lemma 2.2

Proof. Our proof follows [24]. Since $f(t)$ is convex function then $\forall t \in \mathbb{R} f(t) = f^{**}(t)$, where

$$f^{**}(t) = \sup_{s \in \mathbb{R}} \{st - \mathfrak{F}(s)\}$$

is the Fenchel conjugate of \mathfrak{F} . By the Fermat's rule, the maximizer s^* satisfies

$$t \in \partial \mathfrak{F}(s^*),$$

i.e.,

$$s^* \in \partial f(t)$$

Plugging the above display with $t = \frac{d\mu_Z}{d\gamma}(x)$ into the definition of f -divergence, we derive (8). \square

B.3 Proof of Theorem 2.1

Proof. Without loss of generality, we assume that $d^* = 1$. For R^* satisfying (2) and any $R \in \mathcal{R}$, we have $R = \rho_{(R, R^*)} R^* + \varepsilon_R$, where $\rho_{(R, R^*)}$ is the correlation coefficient between

Table 12: Architecture for MNIST, reduced feature size is d^*

Layers	Details	Output size
Convolution	3×3 Conv	$24 \times 28 \times 28$
Dense Block 1	$\begin{bmatrix} \text{BN, } 1 \times 1 \text{ Conv} \\ \text{BN, } 3 \times 3 \text{ Conv} \end{bmatrix} \times 2$	$48 \times 28 \times 28$
Transition Layer 1	BN, ReLU, 2×2 Average Pool, 1×1 Conv	$24 \times 14 \times 14$
Dense Block 2	$\begin{bmatrix} \text{BN, } 1 \times 1 \text{ Conv} \\ \text{BN, } 3 \times 3 \text{ Conv} \end{bmatrix} \times 2$	$48 \times 14 \times 14$
Transition Layer 2	BN, ReLU, 2×2 Average Pool, 1×1 Conv	$24 \times 7 \times 7$
Dense Block 3	$\begin{bmatrix} \text{BN, } 1 \times 1 \text{ Conv} \\ \text{BN, } 3 \times 3 \text{ Conv} \end{bmatrix} \times 2$	$48 \times 7 \times 7$
Pooling	BN, ReLU, 7×7 Average Pool, Reshape	48
Fully connected	Linear	d^*

Table 13: Architecture for FashionMNIST, reduced feature size is d^*

Layers	Details	Output size
Convolution	3×3 Conv	$24 \times 28 \times 28$
Dense Block 1	$\begin{bmatrix} \text{BN, } 1 \times 1 \text{ Conv} \\ \text{BN, } 3 \times 3 \text{ Conv} \end{bmatrix} \times 16$	$216 \times 28 \times 28$
Transition Layer 1	BN, ReLU, 2×2 Average Pool, 1×1 Conv	$108 \times 14 \times 14$
Dense Block 2	$\begin{bmatrix} \text{BN, } 1 \times 1 \text{ Conv} \\ \text{BN, } 3 \times 3 \text{ Conv} \end{bmatrix} \times 16$	$300 \times 14 \times 14$
Transition Layer 2	BN, ReLU, 2×2 Average Pool, 1×1 Conv	$150 \times 7 \times 7$
Dense Block 3	$\begin{bmatrix} \text{BN, } 1 \times 1 \text{ Conv} \\ \text{BN, } 3 \times 3 \text{ Conv} \end{bmatrix} \times 16$	$342 \times 7 \times 7$
Pooling	BN, ReLU, 7×7 Average Pool, Reshape	342
Fully connected	Linear	d^*

Table 14: Architecture for CIFAR-10, reduced feature size is d^*

Layers	Details	Output size
Convolution	3×3 Conv	$24 \times 32 \times 32$
Dense Block 1	$\begin{bmatrix} \text{BN, } 1 \times 1 \text{ Conv} \\ \text{BN, } 3 \times 3 \text{ Conv} \end{bmatrix} \times 16$	$216 \times 32 \times 32$
Transition Layer 1	BN, ReLU, 2×2 Average Pool, 1×1 Conv	$108 \times 16 \times 16$
Dense Block 2	$\begin{bmatrix} \text{BN, } 1 \times 1 \text{ Conv} \\ \text{BN, } 3 \times 3 \text{ Conv} \end{bmatrix} \times 16$	$300 \times 16 \times 16$
Transition Layer 2	BN, ReLU, 2×2 Average Pool, 1×1 Conv	$150 \times 8 \times 8$
Dense Block 3	$\begin{bmatrix} \text{BN, } 1 \times 1 \text{ Conv} \\ \text{BN, } 3 \times 3 \text{ Conv} \end{bmatrix} \times 16$	$342 \times 8 \times 8$
Pooling	BN, ReLU, 8×8 Average Pool, Reshape	342
Fully connected	Linear	d^*

R and R^* , $\varepsilon_R = R - \rho_{(R,R^*)}R^*$. It is easy to see that $\varepsilon_R \perp R^*$ and thus $Y \perp \varepsilon_R$. As $(\rho_{(R,R^*)}R^*, Y)$ is independent of $(\varepsilon_R, 0)$, then by Theorem 3 of [49]

$$\begin{aligned} \mathcal{V}^2(R, Y) &= \mathcal{V}^2(\rho_{(R,R^*)}R^* + \varepsilon_R, Y) \leq \mathcal{V}^2(\rho_{(R,R^*)}R^*, Y) + \mathcal{V}^2(\varepsilon_R, 0) \\ &= \mathcal{V}^2(\rho_{(R,R^*)}R^*, Y) = |\rho_{(R,R^*)}| \mathcal{V}^2(R^*, Y) \\ &\leq \mathcal{V}^2(R^*, Y). \end{aligned}$$

As $R(X) \sim \mathcal{N}(0, 1)$ and $R^*(X) \sim \mathcal{N}(0, 1)$, then $\mathbb{D}_f(\mu_{R(X)} \parallel \gamma_{d^*}) = \mathbb{D}_f(\mu_{R^*(X)} \parallel \gamma_{d^*}) = 0$, and

$$\mathcal{L}(R) - \mathcal{L}(R^*) = \lambda \mathcal{V}^2(R^*, Y) - \lambda \mathcal{V}^2(R, Y) \geq 0.$$

The proof is completed. □

B.4 Proof of Theorem 2.2

Proof. Without loss of generality, we assume that $\lambda = 1$. First we consider the scenario that Y is bounded almost surely, say $|Y| \leq C_1$. We also assume $B_1 < \infty$. We can utilize the truncation technique to transfer the unbounded cases into the bounded ones under some common tail assumptions. As consequence, additional $\log n$ term will appear in the final results. $\forall \bar{R} \in \mathcal{N}_{\mathcal{D}, \mathcal{W}, \mathcal{S}, \mathcal{B}}$ we have,

$$\begin{aligned} \mathcal{L}(\hat{R}_\theta) - \mathcal{L}(R^*) &= \mathcal{L}(\hat{R}_\theta) - \hat{\mathcal{L}}(\hat{R}_\theta) + \hat{\mathcal{L}}(\hat{R}_\theta) - \hat{\mathcal{L}}(\bar{R}) + \hat{\mathcal{L}}(\bar{R}) - \mathcal{L}(\bar{R}) + \mathcal{L}(\bar{R}) - \mathcal{L}(R^*) \\ &\leq 2 \sup_{R \in \mathcal{N}_{\mathcal{D}, \mathcal{W}, \mathcal{S}, \mathcal{B}}} |\mathcal{L}(R) - \hat{\mathcal{L}}(R)| + \inf_{\bar{R} \in \mathcal{N}_{\mathcal{D}, \mathcal{W}, \mathcal{S}, \mathcal{B}}} |\mathcal{L}(\bar{R}) - \mathcal{L}(R^*)| \end{aligned} \quad (13)$$

where we use the definition of \widehat{R}_θ in (10) and the feasibility of \bar{R} . Next we bound the two errors in (13), i.e., approximation error $\inf_{\bar{R} \in \mathcal{N}_{\mathcal{D}, \mathcal{W}, \mathcal{S}, \mathcal{B}}} |\mathcal{L}(\bar{R}) - \mathcal{L}(R^*)|$ and statistical error $\sup_{R \in \mathcal{N}_{\mathcal{D}, \mathcal{W}, \mathcal{S}, \mathcal{B}}} |\mathcal{L}(R) - \widehat{\mathcal{L}}(R)|$, respectively. And we will complete the proof after bounding these two errors.

Approximation error

Lemma B.1.

$$\inf_{\bar{R} \in \mathcal{N}_{\mathcal{D}, \mathcal{W}, \mathcal{S}, \mathcal{B}}} |\mathcal{L}(\bar{R}) - \mathcal{L}(R^*)| \leq 2600C_1 B_1 L_1 \sqrt{dd^*} n^{-\frac{2}{d+2}}. \quad (14)$$

Proof. By (2) and (8) and the definition of \mathcal{L} , we have

$$\inf_{\bar{R} \in \mathcal{N}_{\mathcal{D}, \mathcal{W}, \mathcal{S}, \mathcal{B}}} |\mathcal{L}(\bar{R}) - \mathcal{L}(R^*)| \leq |\mathbb{D}_f(\mu_{\bar{R}_{\bar{\theta}}(X)} \|\gamma_{d^*})| + |\mathcal{V}^2(R^*(X), Y) - \mathcal{V}^2(\bar{R}_{\bar{\theta}}(X), Y)|, \quad (15)$$

where $\bar{R}_{\bar{\theta}} \in \mathcal{N}_{\mathcal{D}, \mathcal{W}, \mathcal{S}, \mathcal{B}}$ is specified in Lemma B.2 below. We finish the proof by (17) in Lemma B.3 and (18) in Lemma B.4, which will be proved below. \square

Lemma B.2. Define $\tilde{R}^*(x) = \min\{R^*(x), \log n\}$. There exist a $\bar{R}_{\bar{\theta}} \in \mathcal{N}_{\mathcal{D}, \mathcal{W}, \mathcal{S}, \mathcal{B}}$ with with depth $\mathcal{D} = 9 \log n + 12$, width $\mathcal{W} = d^* \max\{8d(n^{\frac{d}{2+d}} / \log n)^{\frac{1}{d}} + 4d, 12n^{\frac{d}{2+d}} / \log n + 14\}$, and size $\mathcal{S} = d^* n^{\frac{d-2}{d+2}} / (\log^4 n d d^*)$, $\mathcal{B} = (2B_1 L_1 \sqrt{d} + \log n) \sqrt{d^*}$, such that

$$\|\bar{R}_{\bar{\theta}} - \tilde{R}^*\|_{L^2(\mu_X)} \leq 160L_1 B_1 \sqrt{dd^*} n^{-\frac{2}{d+2}}. \quad (16)$$

Proof. Let $\tilde{R}_i^*(x)$ be the i -th entry of $\tilde{R}^*(x) : \mathbb{R}^d \rightarrow \mathbb{R}^{d^*}$. By the assumption of R^* , it is easy to deduce that $\tilde{R}_i^*(x)$ is Lipschitz continuous on $[-B_1, B_1]^d$ with Lipschitz constant L_1 and $\|\tilde{R}_i^*\|_{L^\infty} \leq \log n$. By Theorem 4.3 in [45], there exist a ReLU network $\bar{R}_{\bar{\theta}_i}$ with with depth $9 \log n + 12$, width $\max\{8d(n^{\frac{d}{2+d}} / \log n)^{\frac{1}{d}} + 4d, 12n^{\frac{d}{2+d}} / \log n + 14\}$, $\|\bar{R}_{\bar{\theta}_i}\|_{L^\infty} = 2B_1 L_1 \sqrt{d} + \log n$, such that

$$\|\bar{R}_{\bar{\theta}_i}\|_{L^\infty} \leq 2B_1 L_1 \sqrt{d} + \log n,$$

and

$$\begin{aligned} \|\tilde{R}_i^* - \bar{R}_{\bar{\theta}_i}\|_{L^\infty([-B_1, B_1]^d \setminus \mathcal{H})} &\leq 80L_1 B_1 \sqrt{dn}^{-\frac{2}{d+2}}, \\ \mu_X(\mathcal{H}) &\leq \frac{80L_1 B_1 \sqrt{dn}^{-\frac{2}{d+2}}}{2B_1 L_1 \sqrt{d} + \log n}. \end{aligned}$$

Define $\bar{R}_{\bar{\theta}} = [\bar{R}_{\bar{\theta}_1}; \dots; \bar{R}_{\bar{\theta}_{d^*}}] \in \mathcal{N}_{\mathcal{D}, \mathcal{W}, \mathcal{S}, \mathcal{B}}$. The above three display implies

$$\|\bar{R}_{\bar{\theta}} - \tilde{R}^*\|_{L^2(\mu_X)} \leq 160L_1 B_1 \sqrt{dd^*} n^{-\frac{2}{d+2}}.$$

\square

Lemma B.3.

$$|\mathcal{V}^2(R^*(X), Y) - \mathcal{V}^2(\bar{R}_{\bar{\theta}}(X), Y)| \leq 2580C_1B_1L_1\sqrt{dd^*}n^{-\frac{2}{d+2}}. \quad (17)$$

Proof. Recall that [51]

$$\begin{aligned} \mathcal{V}^2(Z, Y) = & \mathbb{E} [\|Z_1 - Z_2\| |Y_1 - Y_2|] - 2\mathbb{E} [\|Z_1 - Z_2\| |Y_1 - Y_3|] \\ & + \mathbb{E} [\|Z_1 - Z_2\|] \mathbb{E} [|Y_1 - Y_2|], \end{aligned}$$

where $(Z_i, Y_i), i = 1, 2, 3$ are i.i.d. copies of (Z, Y) . We have

$$\begin{aligned} & |\mathcal{V}^2(R^*(X), Y) - \mathcal{V}^2(\bar{R}_{\bar{\theta}}(X), Y)| \\ & \leq \mathbb{E} [(\|R^*(X_1) - R^*(X_2)\| - \|\bar{R}_{\bar{\theta}}(X_1) - \bar{R}_{\bar{\theta}}(X_2)\|) |Y_1 - Y_2|] | \\ & + 2\mathbb{E} [(\|R^*(X_1) - R^*(X_2)\| - \|\bar{R}_{\bar{\theta}}(X_1) - \bar{R}_{\bar{\theta}}(X_2)\|) |Y_1 - Y_3|] | \\ & + \mathbb{E} [\|R^*(X_1) - R^*(X_2)\| - \|\bar{R}_{\bar{\theta}}(X_1) - \bar{R}_{\bar{\theta}}(X_2)\|] \mathbb{E} [|Y_1 - Y_2|] | \\ & \leq 8C_1\mathbb{E} [\|R^*(X_1) - R^*(X_2)\| - \|\bar{R}_{\bar{\theta}}(X_1) - \bar{R}_{\bar{\theta}}(X_2)\|] \\ & \leq 16C_1\mathbb{E} [\|R^*(X) - \bar{R}_{\bar{\theta}}(X)\|] \\ & \leq 16C_1(\mathbb{E} [\|\tilde{R}^*(X) - \bar{R}_{\bar{\theta}}(X)\|] + \mathbb{E} [\|R^*(X)\mathbf{1}_{R^*(X) \in \text{Ball}^c(\mathbf{0}, \log n)}\|]), \end{aligned}$$

where in the first and third inequalities we use triangle inequality, and second one follows from the boundness of Y . By (16), the first term in last line is bounded by $2560C_1B_1L_1\sqrt{dd^*}n^{-\frac{1}{d+2}}$. Some direct calculation implies that

$$\mathbb{E} [\|R^*(X)\mathbf{1}_{R^*(X) \in \text{Ball}^c(\mathbf{0}, \log n)}\|] \leq C_2 \frac{(\log n)^{d^*}}{n}.$$

We finish the proof by comparing the order of the above two terms, i.e., $C_2 \frac{(\log n)^{d^*}}{n} \leq 20C_1B_1L_1\sqrt{dd^*}n^{-\frac{2}{d+2}}$. \square

Lemma B.4.

$$|\mathbb{D}_f(\mu_{\bar{R}_{\bar{\theta}}(X)} \| \gamma_{d^*})| \leq 20C_1B_1L_1\sqrt{dd^*}n^{-\frac{2}{d+2}}. \quad (18)$$

Proof. By Lemma B.2 $\bar{R}_{\bar{\theta}}$ can approximate R^* arbitrary well, the desired result follows from the fact that $\mathbb{D}_f(\mu_{R^*(X)} \| \gamma_{d^*}) = 0$ and the continuity of $\mathbb{D}_f(\mu_{R(X)} \| \gamma_{d^*})$ on R . We present the sketch of the proof and omit the detail here. Let $r^*(z) = \frac{d\mu_{R^*(X)}}{d\gamma_{d^*}}(z)$ and $\bar{r}(z) = \frac{d\mu_{\bar{R}_{\bar{\theta}}(X)}}{d\gamma_{d^*}}(z)$. By definition we have

$$\begin{aligned} \mathbb{D}_f(\mu_{R^*(X)} \| \gamma_{d^*}) &= \mathbb{E}_{W \sim \gamma_{d^*}} [f(r^*(W))] \\ &= \mathbb{E}_{W \sim \gamma_{d^*}} [f(r^*(W))\mathbf{1}_{W \in \text{Ball}(0, \log n)}] + \mathbb{E}_{W \sim \gamma_{d^*}} [f(r^*(W))\mathbf{1}_{W \in \text{Ball}^c(0, \log n)}]. \end{aligned}$$

(We can represent $\mathbb{D}_f(\mu_{\bar{R}_\theta}||\gamma_{d^*})$ similarly.) Then

$$\begin{aligned}
|\mathbb{D}_f(\mu_{\bar{R}_\theta(X)}||\gamma_{d^*})| &= |\mathbb{D}_f(\mu_{\bar{R}_\theta(X)}||\gamma_{d^*}) - \mathbb{D}_f(\mu_{R^*(X)}||\gamma_{d^*})| \\
&\leq \mathbb{E}_{W \sim \gamma_{d^*}} [|f(r^*(W)) - f(\bar{r}(W))| \mathbf{1}_{W \in \text{Ball}(0, \log n)}] \\
&\quad + \mathbb{E}_{W \sim \gamma_{d^*}} [|f(r^*(W)) - f(r^*(W))| \mathbf{1}_{W \in \text{Ball}^c(0, \log n)}] \\
&\leq \int_{\|z\| \leq \log n} |f'(\bar{r}(z))| |r^*(z) - \bar{r}(z)| d\gamma_{d^*}(z) + \int_{\|z\| > \log n} |f'(\bar{r}(z))| |r^*(z) - \bar{r}(z)| d\gamma_{d^*}(z) \\
&\leq C_3 \int_{\|z\| \leq \log n} |r^*(z) - \bar{r}(z)| d\gamma_{d^*}(z) + C_4 \int_{\|z\| > \log n} |r^*(z) - \bar{r}(z)|
\end{aligned}$$

The first term in the above display is small due to \bar{R}_θ can approximate R^* well. The second term is small due to the boundedness of \bar{r} and the exponential decay of Gaussian tail. \square

Statistical error

Lemma B.5.

$$\sup_{R \in \mathcal{N}_{\mathcal{D}, \mathcal{W}, \mathcal{S}, \mathcal{B}}} |\mathcal{L}(R) - \hat{\mathcal{L}}(R)| \leq C_{15} (B_1(L_1 + L_2) \sqrt{dd^*}) n^{-\frac{2}{2+d}} + (L_2 \sqrt{d^*} + B_2 + B_3) \log nn^{-\frac{2}{2+d^*}} \quad (19)$$

Proof. By definition and triangle inequality we have

$$\begin{aligned}
&\mathbb{E} \left[\sup_{R \in \mathcal{N}_{\mathcal{D}, \mathcal{W}, \mathcal{S}, \mathcal{B}}} |\mathcal{L}(R) - \hat{\mathcal{L}}(R)| \right] \\
&\leq \mathbb{E} \left[\sup_{R \in \mathcal{N}_{\mathcal{D}, \mathcal{W}, \mathcal{S}, \mathcal{B}}} |\hat{\mathcal{V}}_n^2(R(X), Y) - \mathcal{V}^2((R(X), Y))| \right] \\
&\quad + \mathbb{E} \left[\sup_{R \in \mathcal{N}_{\mathcal{D}, \mathcal{W}, \mathcal{S}, \mathcal{B}}} |\hat{\mathbb{D}}_f(\mu_{R(X)}||\gamma_{d^*}) - \mathbb{D}_f(\mu_{R(X)}||\gamma_{d^*})| \right].
\end{aligned}$$

We finish the proof by (20) in Lemma B.6 and (25) in Lemma B.8, which will be proved below. \square

Lemma B.6.

$$\mathbb{E} \left[\sup_{R \in \mathcal{N}_{\mathcal{D}, \mathcal{W}, \mathcal{S}, \mathcal{B}}} |\hat{\mathcal{V}}_n^2(R(X), Y) - \mathcal{V}^2((R(X), Y))| \right] \leq 4C_6 C_7 C_{10} B_1 L_1 \sqrt{dd^*} n^{-\frac{2}{d+2}}. \quad (20)$$

Proof. We first fix some notation for simplicity. Denote $O = (X, Y) \in \mathbb{R}^d \times \mathbb{R}^1$ and $O_i = (X_i, Y_i), i = 1, \dots, n$ are i.i.d copy of O , and denote $\mu_{X, Y}$ and $\mathbb{P}^{\otimes n}$ as \mathbb{P} and \mathbb{P}^n , respectively. $\forall R \in \mathcal{N}_{\mathcal{D}, \mathcal{W}, \mathcal{S}, \mathcal{B}}$, let $\tilde{O} = (R(X), Y)$ and $\tilde{O}_i = (R(X_i), Y_i), i = 1, \dots, n$ are i.i.d

copy of \tilde{O} . Define centered kernel $\bar{h}_R : (\mathbb{R}^d \times \mathbb{R}^1)^{\otimes 4} \rightarrow \mathbb{R}$ as

$$\begin{aligned} \bar{h}_R(\tilde{O}_1, \tilde{O}_2, \tilde{O}_3, \tilde{O}_4) &= \frac{1}{4} \sum_{\substack{1 \leq i, j \leq 4 \\ i \neq j}} \|R(X_i) - R(X_j)\| |Y_i - Y_j| \\ &- \frac{1}{4} \sum_{i=1}^4 \left(\sum_{\substack{1 \leq j \leq 4 \\ j \neq i}} \|R(X_i) - R(X_j)\| \sum_{\substack{1 \leq j \leq 4 \\ i \neq j}} |Y_i - Y_j| \right) \\ &+ \frac{1}{24} \sum_{\substack{1 \leq i, j \leq 4 \\ i \neq j}} \|R(X_i) - R(X_j)\| \sum_{\substack{1 \leq i, j \leq 4 \\ i \neq j}} |Y_i - Y_j| - \mathcal{V}^2((R(X), Y)) \end{aligned} \quad (21)$$

Then, the centered U -statistics $\hat{\mathcal{V}}_n^2(R(X), Y) - \mathcal{V}^2((R(X), Y))$ can be represented as

$$\mathbb{U}_n(\bar{h}_R) = \frac{1}{C_n^4} \sum_{1 \leq i_1 < i_2 < i_3 < i_4 \leq n} \bar{h}_R(\tilde{O}_{i_1}, \tilde{O}_{i_2}, \tilde{O}_{i_3}, \tilde{O}_{i_4}).$$

And our goal is to bound the supremum of centner U -process $\mathbb{U}_n(\bar{h}_R)$ with nondegenerate kernel \bar{h}_R . By the symmetrization randomization Theorem 3.5.3 in [13], we have

$$\mathbb{E} \left[\sup_{R \in \mathcal{N}_{\mathcal{D}, \mathcal{W}, \mathcal{S}, \mathcal{B}}} |\mathbb{U}_n(\bar{h}_R)| \right] \leq C_5 \mathbb{E} \left[\sup_{R \in \mathcal{N}_{\mathcal{D}, \mathcal{W}, \mathcal{S}, \mathcal{B}}} \left| \frac{1}{C_n^4} \sum_{1 \leq i_1 < i_2 < i_3 < i_4 \leq n} \epsilon_{i_1} \bar{h}_R(\tilde{O}_{i_1}, \tilde{O}_{i_2}, \tilde{O}_{i_3}, \tilde{O}_{i_4}) \right| \right], \quad (22)$$

where, $\epsilon_{i_1}, i_1 = 1, \dots, n$ are i.i.d Rademacher variables that are also independent with $\tilde{O}_i, i = 1, \dots, n$. We finish the proof by upper bound the above Rademacher process with the matrix entropy of $\mathcal{N}_{\mathcal{D}, \mathcal{W}, \mathcal{S}, \mathcal{B}}$. To this end we need the following results.

Lemma B.7. B.8 So, if $\xi_i, i = 1, \dots, m$ are m finite linear combinations of Rademacher variables $\epsilon_j, j = 1, \dots, J$. Then

$$\mathbb{E}_{\epsilon_j, j=1, \dots, J} \max_{1 \leq i \leq m} |\xi_i| \leq C_6 (\log m)^{1/2} \max_{1 \leq i \leq m} (\mathbb{E} \xi_i^2)^{1/2}. \quad (23)$$

Proof. This result follows directly from Corollary 3.2.6 and inequality (4.3.1) in [13] with $\Phi(x) = \exp(x^2)$. \square

By the bounded assumption on Y and the boundedness of $R \in \mathcal{N}_{\mathcal{D}, \mathcal{W}, \mathcal{S}, \mathcal{B}}$, we get the kernel \bar{h}_R is also bounded, say

$$\|\bar{h}_R\|_{L^\infty} \leq C_7 (2B_1 L_1 \sqrt{d} + \log n) \sqrt{d^*}. \quad (24)$$

$\forall R, \tilde{R} \in \mathcal{N}_{\mathcal{D}, \mathcal{W}, \mathcal{S}, \mathcal{B}}$ define a random empirical measure (depends on $O_i, i = 1, \dots, n$)

$$e_{n,1}(R, \tilde{R}) = \mathbb{E}_{\epsilon_{i_1}, i_1=1, \dots, n} \left| \frac{1}{C_n^4} \sum_{1 \leq i_1 < i_2 < i_3 < i_4 \leq n} \epsilon_{i_1} (\bar{h}_R - \bar{h}_{\tilde{R}})(\tilde{O}_{i_1}, \dots, \tilde{O}_{i_4}) \right|.$$

Condition on $O_i, i = 1, \dots, n$, let $\mathfrak{C}(\mathcal{N}, e_{n,1}, \delta)$ be the covering number of $\mathcal{N}_{\mathcal{D}, \mathcal{W}, \mathcal{S}, \mathcal{B}}$ with respect the empirical distance $e_{n,1}$ at scale of $\delta > 0$. Denote \mathcal{N}_δ as the covering set of

$\mathcal{N}_{\mathcal{D}, \mathcal{W}, \mathcal{S}, \mathcal{B}}$ with cardinality of $\mathfrak{C}(\mathcal{N}, e_{n,1}, \delta)$. Then,

$$\begin{aligned}
& \mathbb{E}_{\epsilon_{i_1}} \left[\sup_{R \in \mathcal{N}_{\mathcal{D}, \mathcal{W}, \mathcal{S}, \mathcal{B}}} \left| \frac{1}{C_n^4} \sum_{1 \leq i_1 < i_2 < i_3 < i_4 \leq n} \epsilon_{i_1} \bar{h}_R(\tilde{O}_{i_1}, \tilde{O}_{i_2}, \tilde{O}_{i_3}, \tilde{O}_{i_4}) \right| \right] \\
& \leq \delta + \mathbb{E}_{\epsilon_{i_1}} \left[\sup_{R \in \mathcal{N}_\tau} \left| \frac{1}{C_n^4} \sum_{1 \leq i_1 < i_2 < i_3 < i_4 \leq n} \epsilon_{i_1} \bar{h}_R(\tilde{O}_{i_1}, \tilde{O}_{i_2}, \tilde{O}_{i_3}, \tilde{O}_{i_4}) \right| \right] \\
& \leq \delta + C_6 \frac{1}{C_n^4} (\log \mathfrak{C}(\mathcal{N}, e_{n,1}, \delta))^{1/2} \max_{R \in \mathcal{N}_\delta} \left[\sum_{i_1=1}^n \sum_{i_2 < i_3 < i_4} (\bar{h}_R(\tilde{O}_{i_1}, \tilde{O}_{i_2}, \tilde{O}_{i_3}, \tilde{O}_{i_4}))^2 \right]^{1/2} \\
& \leq \delta + C_6 C_7 (2B_1 L_1 \sqrt{d} + \log n) \sqrt{d^*} (\log \mathfrak{C}(\mathcal{N}, e_{n,1}, \delta))^{1/2} \frac{1}{C_n^4} \left[\frac{n(n!)^2}{((n-3)!)^2} \right]^{1/2} \\
& \leq \delta + 2C_6 C_7 (2B_1 L_1 \sqrt{d} + \log n) \sqrt{d^*} (\log \mathfrak{C}(\mathcal{N}, e_{n,1}, \delta))^{1/2} / \sqrt{n} \\
& \leq \delta + 2C_6 C_7 (2B_1 L_1 \sqrt{d} + \log n) \sqrt{d^*} (\text{VC}_{\mathcal{N}} \log \frac{2e\mathcal{B}n}{\delta \text{VC}_{\mathcal{N}}})^{1/2} / \sqrt{n} \\
& \leq \delta + C_6 C_7 C_{10} (B_1 L_1 \sqrt{d} + \log n) \sqrt{d^*} (\mathcal{D}\mathcal{S} \log \mathcal{S} \log \frac{\mathcal{B}n}{\delta \mathcal{D}\mathcal{S} \log \mathcal{S}})^{1/2} / \sqrt{n}.
\end{aligned}$$

where, the first inequality follows from triangle inequality, and the second inequality uses (23), and the third and fourth inequalities holds after some algebra, and the fifth inequality holds due to $\mathfrak{C}(\mathcal{N}, e_{n,1}, \delta) \leq \mathfrak{C}(\mathcal{N}, e_{n,\infty}, \delta)$ and the relationship between the matric entropy and the VC-dimension of the ReLU networks $\mathcal{N}_{\mathcal{D}, \mathcal{W}, \mathcal{S}, \mathcal{B}}$ [6], i.e.,

$$\log \mathfrak{C}(\mathcal{N}, e_{n,\infty}, \delta) \leq \text{VC}_{\mathcal{N}} \log \frac{2e\mathcal{B}n}{\delta \text{VC}_{\mathcal{N}}},$$

and the last inequality holds due to the upper bound of VC-dimension for the ReLU network $\mathcal{N}_{\mathcal{D}, \mathcal{W}, \mathcal{S}, \mathcal{B}}$ satisfying

$$C_8 \mathcal{D}\mathcal{S} \log \mathcal{S} \leq \text{VC}_{\mathcal{N}} \leq C_9 \mathcal{D}\mathcal{S} \log \mathcal{S},$$

see [7]. Then (20) holds by the selection of network parameters and set $\delta = \frac{1}{n}$ and some algebra. \square

Lemma B.8.

$$\mathbb{E} \left[\sup_{R \in \mathcal{N}_{\mathcal{D}, \mathcal{W}, \mathcal{S}, \mathcal{B}}} \left| \widehat{\mathbb{D}}_f(\mu_{R(X)} || \gamma_{d^*}) - \mathbb{D}_f(\mu_{R(X)} || \gamma_{d^*}) \right| \right] \leq C_{14} (L_2 \sqrt{d^*} + B_2 + B_3) (n^{-\frac{2}{2+d^*}} + \log n n^{-\frac{2}{2+d^*}}) \quad (25)$$

Proof. $\forall R \in \mathcal{N}_{\mathcal{D}, \mathcal{W}, \mathcal{S}, \mathcal{B}}$, let $r(z) = \frac{d\mu_{R(X)}}{d\gamma_{d^*}}(z)$, $g_R(z) = f'(r(z))$. By assumption $g_R(z) : \mathbb{R}^{d^*} \rightarrow \mathbb{R}$ is Lipschitz continuous with Lipschitz constant L_2 and $\|g_R\|_{L^\infty} \leq B_2$. Without loss of generality, we assume $\text{supp}(g_R) \subseteq [-\log n, \log n]^{d^*}$. Then, similar as the proof of Lemma B.2 we can prove that there exist a $\bar{D}_{\bar{\phi}} \in \mathcal{M}_{\bar{\mathcal{D}}, \bar{\mathcal{W}}, \bar{\mathcal{S}}, \bar{\mathcal{B}}}$ with depth $\bar{\mathcal{D}} = 9 \log n + 12$, width $\bar{\mathcal{W}} = \max\{8d^* (n^{\frac{d^*}{2+d^*}} / \log n)^{\frac{1}{d^*}} + 4d^*, 12n^{\frac{d^*}{2+d^*}} / \log n + 14\}$, and size $\bar{\mathcal{S}} = n^{\frac{d^* - 2}{d^* + 2}} / (\log^4 n d d^*)$,

$\tilde{B} = 2L_2\sqrt{d^*} \log n + B_2$ such that for $Z \sim \gamma_{d^*}$ and $Z \sim \mu_{R(X)}$

$$\mathbb{E}_Z[|\bar{D}_{\tilde{\phi}}(Z) - g_R(Z)|] \leq 160L_2\sqrt{d^*} \log nn^{-\frac{2}{d^*+2}}. \quad (26)$$

$\forall g : \mathbb{R}^{d^*} \rightarrow \mathbb{R}$, define

$$\mathcal{E}(g) = \mathbb{E}_{X \sim \mu_X}[g(R(X))] - \mathbb{E}_{W \sim \gamma_{d^*}}[\mathfrak{F}(g(W))],$$

$$\hat{\mathcal{E}}(g) = \hat{\mathcal{E}}(g, R) = \frac{1}{n} \sum_{i=1}^n [g(R(X_i)) - \mathfrak{F}(g(W_i))].$$

By (8) we have

$$\mathcal{E}(g_R) = \mathbb{D}_f(\mu_{R(X)} || \gamma_{d^*}) = \sup_{\text{measurable } D: \mathbb{R}^{d^*} \rightarrow \mathbb{R}} \mathcal{E}(D). \quad (27)$$

Then,

$$\begin{aligned} & |\mathbb{D}_f(\mu_{R(X)} || \gamma_{d^*}) - \hat{\mathbb{D}}_f(\mu_{R(X)} || \gamma_{d^*})| \\ &= |\mathcal{E}(g_R) - \max_{D_\phi \in \mathcal{M}_{\bar{D}, \bar{W}, \bar{S}, \bar{B}}} \hat{\mathcal{E}}(D_\phi)| \\ &\leq |\mathcal{E}(g_R) - \sup_{D_\phi \in \mathcal{M}_{\bar{D}, \bar{W}, \bar{S}, \bar{B}}} \mathcal{E}(D_\phi)| + |\sup_{D_\phi \in \mathcal{M}_{\bar{D}, \bar{W}, \bar{S}, \bar{B}}} \mathcal{E}(D_\phi) - \max_{D_\phi \in \mathcal{M}_{\bar{D}, \bar{W}, \bar{S}, \bar{B}}} \hat{\mathcal{E}}(D_\phi)| \\ &\leq |\mathcal{E}(g_R) - \mathcal{E}(\bar{D}_{\tilde{\phi}})| + \sup_{D_\phi \in \mathcal{M}_{\bar{D}, \bar{W}, \bar{S}, \bar{B}}} |\mathcal{E}(D_\phi) - \hat{\mathcal{E}}(D_\phi)| \\ &\leq \mathbb{E}_{Z \sim \mu_{R(X)}}[|g_R - \bar{D}_{\tilde{\phi}}|(Z)] + \mathbb{E}_{W \sim \gamma_{d^*}}[|\mathfrak{F}(g_R) - \mathfrak{F}(\bar{D}_{\tilde{\phi}})(W)|] + \sup_{D_\phi \in \mathcal{M}_{\bar{D}, \bar{W}, \bar{S}, \bar{B}}} |\mathcal{E}(D_\phi) - \hat{\mathcal{E}}(D_\phi)| \\ &\leq 160(1 + B_3)L_2\sqrt{d^*} \log nn^{-\frac{2}{d^*+2}} + \sup_{D_\phi \in \mathcal{M}_{\bar{D}, \bar{W}, \bar{S}, \bar{B}}} |\mathcal{E}(D_\phi) - \hat{\mathcal{E}}(D_\phi)| \end{aligned}$$

where, we use triangle inequality in the first inequality, and we use $\mathcal{E}(g_R) \geq \sup_{D_\phi \in \mathcal{M}_{\bar{D}, \bar{W}, \bar{S}, \bar{B}}} \mathcal{E}(D_\phi)$ followed from (27) and triangle inequality in the second inequality, the third inequality follows from triangle inequality, and the last inequality follows from (26) and mean value Theorem. We will finish the proof via bounding the empirical process

$$\mathbb{U}(D, R) = \mathbb{E}[\sup_{R \in \mathcal{N}_{\mathcal{D}, \mathcal{W}, \mathcal{S}, \mathcal{B}}, D \in \mathcal{M}_{\bar{D}, \bar{W}, \bar{S}, \bar{B}}} |\mathcal{E}(D) - \hat{\mathcal{E}}(D)|].$$

Let $S = (X, W) \sim \mu_X \otimes \gamma_{d^*}$ and $S_i, i = 1, \dots, n$ be n i.i.d copy of S . Denote

$$b(D, R; S) = D(R(X)) - \mathfrak{F}(D(W)).$$

Then

$$\mathcal{E}(D, R) = \mathbb{E}_S[b(D, R; S)]$$

and

$$\widehat{\mathcal{E}}(D, R) = \frac{1}{n} \sum_{i=1}^n b(D, R; S_i).$$

Let

$$\mathcal{G}(\mathcal{M} \times \mathcal{N}) = \frac{1}{n} \mathbb{E}_{\{S_i, \epsilon_i\}_i^n} \left[\sup_{R \in \mathcal{N}_{\mathcal{D}, \mathcal{W}, \mathcal{S}, \mathcal{B}}, D \in \mathcal{M}_{\tilde{\mathcal{D}}, \tilde{\mathcal{W}}, \tilde{\mathcal{S}}, \tilde{\mathcal{B}}}} \left| \sum_{i=1}^n \epsilon_i b(D, R; S_i) \right| \right]$$

be the Rademacher complexity of $\mathcal{M}_{\tilde{\mathcal{D}}, \tilde{\mathcal{W}}, \tilde{\mathcal{S}}, \tilde{\mathcal{B}}} \times \mathcal{N}_{\mathcal{D}, \mathcal{W}, \mathcal{S}, \mathcal{B}}$ [8]. Let $\mathfrak{C}(\mathcal{M} \times \mathcal{N}, d_{n,1}, \delta)$ be the covering number of $\mathcal{M}_{\tilde{\mathcal{D}}, \tilde{\mathcal{W}}, \tilde{\mathcal{S}}, \tilde{\mathcal{B}}} \times \mathcal{N}_{\mathcal{D}, \mathcal{W}, \mathcal{S}, \mathcal{B}}$ with respect the empirical distance (depends on S_i)

$$d_{n,1}((D, R), (\tilde{D}, \tilde{R})) = \frac{1}{n} \mathbb{E}_{\epsilon_i} \left[\sum_{i=1}^n |\epsilon_i (b(D, R; S_i) - b(\tilde{D}, \tilde{R}; S_i))| \right]$$

at scale of $\delta > 0$. Let $\mathcal{M}_\delta \times \mathcal{N}_\delta$ be the such converging set of $\mathcal{M}_{\tilde{\mathcal{D}}, \tilde{\mathcal{W}}, \tilde{\mathcal{S}}, \tilde{\mathcal{B}}} \times \mathcal{N}_{\mathcal{D}, \mathcal{W}, \mathcal{S}, \mathcal{B}}$. Then,

$$\begin{aligned} \mathbb{U}(D, R) &= 2\mathcal{R}(\mathcal{M} \times \mathcal{N}) \\ &= 2\mathbb{E}_{S_1, \dots, S_n} [\mathbb{E}_{\epsilon_i, i=1, \dots, n} [\mathcal{R}(\mathcal{N} \times \mathcal{M})|(S_1, \dots, S_n)]] \\ &\leq 2\delta + \frac{2}{n} \mathbb{E}_{S_1, \dots, S_n} [\mathbb{E}_{\epsilon_i, i=1, \dots, n} \left[\sup_{(D, R) \in \mathcal{M}_\delta \times \mathcal{N}_\delta} \left| \sum_{i=1}^n \epsilon_i b(D, R; S_i) \right| |(S_1, \dots, S_n) \right]] \\ &\leq 2\delta + C_{12} \frac{1}{n} \mathbb{E}_{S_1, \dots, S_n} [(\log \mathfrak{C}(\mathcal{M} \times \mathcal{N}, d_{n,1}, \delta))^{1/2} \max_{(D, R) \in \mathcal{M}_\delta \times \mathcal{N}_\delta} \left[\sum_{i=1}^n b^2(D, R; S_i) \right]^{1/2}] \\ &\leq 2\delta + C_{12} \frac{1}{n} \mathbb{E}_{S_1, \dots, S_n} [(\log \mathfrak{C}(\mathcal{M} \times \mathcal{N}, d_{n,1}, \delta))^{1/2} \sqrt{n} (2L_2 \sqrt{d^*} \log n + B_2 + B_3)] \\ &\leq 2\delta + C_{12} \frac{1}{\sqrt{n}} (2L_2 \sqrt{d^*} \log n + B_2 + B_3) (\log \mathfrak{C}(\mathcal{M}, d_{n,1}, \delta) + \log \mathfrak{C}(\mathcal{N}, d_{n,1}, \delta))^{1/2} \\ &\leq 2\delta + C_{13} \frac{L_2 \sqrt{d^*} \log n + B_2 + B_3}{\sqrt{n}} \left(\mathcal{D}\mathcal{S} \log \mathcal{S} \log \frac{\mathcal{B}n}{\delta \mathcal{D}\mathcal{S} \log \mathcal{S}} + \tilde{\mathcal{D}}\tilde{\mathcal{S}} \log \tilde{\mathcal{S}} \log \frac{\tilde{\mathcal{B}}n}{\delta \tilde{\mathcal{D}}\tilde{\mathcal{S}} \log \tilde{\mathcal{S}}} \right)^{1/2} \end{aligned}$$

where first equality follows from the standard symmetrization technique, and the second equality holds due to the iteration law of conditional expectation, and the first inequality uses triangle inequality, and the second inequality uses Lemma B.8, and the third inequality uses the fact that $b(D, R; S)$ is bounded, i.e., $\|b(D, R; S)\|_{L^\infty} \leq 2L_2 \sqrt{d^*} \log n + B_2 + B_3$, and the fourth inequality is some algebra, and the fifth inequality follows from $\mathfrak{C}(\mathcal{N}, d_{n,1}, \delta) \leq \mathfrak{C}(\mathcal{N}, d_{n,\infty}, \delta)$ (similar result for \mathcal{M}) and $\log \mathfrak{C}(\mathcal{N}, d_{n,\infty}, \delta) \leq \text{VC}_{\mathcal{N}} \log \frac{2e\mathcal{B}n}{\delta \text{VC}_{\mathcal{N}}}$, and $\mathcal{N}_{\mathcal{D}, \mathcal{W}, \mathcal{S}, \mathcal{B}}$ satisfying $C_8 \mathcal{D}\mathcal{S} \log \mathcal{S} \leq \text{VC}_{\mathcal{N}} \leq C_9 \mathcal{D}\mathcal{S} \log \mathcal{S}$, see [7]. Then (25) follows from the above display with the selection of network parameters of $\mathcal{M}_{\tilde{\mathcal{D}}, \tilde{\mathcal{W}}, \tilde{\mathcal{S}}, \tilde{\mathcal{B}}}$, $\mathcal{N}_{\mathcal{D}, \mathcal{W}, \mathcal{S}, \mathcal{B}}$ and with $\delta = \frac{1}{n}$. \square

The final desired result is a direct consequence of (14) in Lemma B.1 and (19) in Lemma B.5. \square

References

- [1] A. Achille and S. Soatto. Emergence of invariance and disentanglement in deep representations. *The Journal of Machine Learning Research*, 19(1):1947–1980, 2018.
- [2] G. Alain and Y. Bengio. Understanding intermediate layers using linear classifier probes. In *ICLR Workshop*, 2017.
- [3] A. A. Alemi, I. Fischer, J. V. Dillon, and K. Murphy. Deep variational information bottleneck. In *ICLR*, 2017.
- [4] S. M. Ali and S. D. Silvey. A general class of coefficients of divergence of one distribution from another. *Journal of the Royal Statistical Society: Series B (Methodological)*, 28(1):131–142, 1966.
- [5] B. Amos and J. Z. Kolter. A PyTorch Implementation of DenseNet. <https://github.com/bamos/densenet.pytorch>. Accessed: [20 Feb 2020].
- [6] M. Anthony and P. L. Bartlett. *Neural network learning: Theoretical foundations*. cambridge university press, 2009.
- [7] P. L. Bartlett, N. Harvey, C. Liaw, and A. Mehrabian. Nearly-tight vc-dimension and pseudodimension bounds for piecewise linear neural networks. *Journal of Machine Learning Research*, 20:1–17, 2019.
- [8] P. L. Bartlett and S. Mendelson. Rademacher and gaussian complexities: Risk bounds and structural results. *Journal of Machine Learning Research*, 3:463–482, 2002.
- [9] Y. Bengio, A. Courville, and P. Vincent. Representation learning: A review and new perspectives. *IEEE transactions on pattern analysis and machine intelligence*, 35(8):1798–1828, 2013.
- [10] Y. Brenier. Polar factorization and monotone rearrangement of vector-valued functions. *Communications on pure and applied mathematics*, 44(4):375–417, 1991.
- [11] R. D. Cook. *Regression graphics: ideas for studying regressions through graphics*, volume 482. 1998.
- [12] R. D. Cook. Fisher lecture: Dimension reduction in regression. *Statistical Science*, 22(1):1–26, 2007.
- [13] V. De la Pena and E. Giné. *Decoupling: from dependence to independence*. Springer Science & Business Media, 2012.
- [14] K. Fukumizu, F. R. Bach, and M. I. Jordan. Dimensionality reduction for supervised learning with reproducing kernel hilbert spaces. *Journal of Machine Learning Research*, 5:73–99, 2004.

- [15] K. Fukumizu, F. R. Bach, M. I. Jordan, et al. Kernel dimension reduction in regression. *The Annals of Statistics*, 37(4):1871–1905, 2009.
- [16] Y. Gao, J. Huang, Y. Jiao, and J. Liu. Learning implicit generative models with theoretical guarantees. *arXiv preprint arXiv:2002.02862*, 2020.
- [17] Y. Gao, Y. Jiao, Y. Wang, Y. Wang, C. Yang, and S. Zhang. Deep generative learning via variational gradient flow. In *ICML*, 2019.
- [18] I. Goodfellow, Y. Bengio, and A. Courville. *Deep learning*. 2016.
- [19] A. Graves, A. Mohamed, and G. Hinton. Speech recognition with deep recurrent neural networks. In *2013 IEEE international conference on acoustics, speech and signal processing*, 2013.
- [20] I. Higgins, L. Matthey, A. Pal, C. Burgess, X. Glorot, M. Botvinick, S. Mohamed, and A. Lerchner. beta-vae: Learning basic visual concepts with a constrained variational framework. In *ICLR*, 2017.
- [21] R. D. Hjelm, A. Fedorov, S. Lavoie-Marchildon, K. Grewal, P. Bachman, A. Trischler, and Y. Bengio. Learning deep representations by mutual information estimation and maximization. In *ICLR*, 2019.
- [22] G. Huang, Z. Liu, L. Van Der Maaten, and K. Q. Weinberger. Densely connected convolutional networks. In *CVPR*, 2017.
- [23] X. Huo and G. J. Székely. Fast computing for distance covariance. *Technometrics*, 58(4):435–447, 2016.
- [24] A. Keziou. Dual representation of φ -divergences and applications. *Comptes rendus mathématique*, 336(10):857–862, 2003.
- [25] H. Kim and A. Mnih. Disentangling by factorising. In *ICML*, 2018.
- [26] D. P. Kingma and J. Ba. Adam: A method for stochastic optimization. *arXiv preprint arXiv:1412.6980*, 2014.
- [27] D. P. Kingma and M. Welling. Auto-encoding variational bayes. In *ICLR*, 2014.
- [28] A. Krizhevsky, G. Hinton, et al. Learning multiple layers of features from tiny images. Technical report, 2009.
- [29] A. Krizhevsky, I. Sutskever, and G. E. Hinton. Imagenet classification with deep convolutional neural networks. In *NIPS*, 2012.
- [30] Y. LeCun, Y. Bengio, and G. Hinton. Deep learning. *nature*, 521(7553):436–444, 2015.

- [31] Y. LeCun, C. Cortes, and C. Burges. Mnist handwritten digit database. *AT&T Labs [Online]*. Available: <http://yann.lecun.com/exdb/mnist>, 2, 2010.
- [32] B. Li. *Sufficient dimension reduction: Methods and applications with R*. 2018.
- [33] B. Li, H. Zha, F. Chiaromonte, et al. Contour regression: a general approach to dimension reduction. *The Annals of Statistics*, 33(4):1580–1616, 2005.
- [34] K.-C. Li. Sliced inverse regression for dimension reduction. *Journal of the American Statistical Association*, 86(414):316–327, 1991.
- [35] K.-C. Li. On principal hessian directions for data visualization and dimension reduction: Another application of stein’s lemma. *Journal of the American Statistical Association*, 87(420):1025–1039, 1992.
- [36] F. Locatello, M. Tschannen, S. Bauer, G. Rätsch, B. Schölkopf, and O. Bachem. Disentangling factors of variation using few labels. In *ICLR*, 2020.
- [37] A. Makhzani, J. Shlens, N. Jaitly, and I. Goodfellow. Adversarial autoencoders. In *ICLR*, 2017.
- [38] R. J. McCann et al. Existence and uniqueness of monotone measure-preserving maps. *Duke Mathematical Journal*, 80(2):309–324, 1995.
- [39] S. Nowozin, B. Cseke, and R. Tomioka. f-gan: Training generative neural samplers using variational divergence minimization. In *NIPS*, 2016.
- [40] A. v. d. Oord, Y. Li, and O. Vinyals. Representation learning with contrastive predictive coding. *arXiv preprint arXiv:1807.03748*, 2018.
- [41] G. Philippis. *Regularity of optimal transport maps and applications*, volume 17. Springer Science & Business Media, 2013.
- [42] R. T. Rockafellar. *Convex analysis*. Number 28. Princeton university press, 1970.
- [43] A. M. Saxe, Y. Bansal, J. Dapello, M. Advani, A. Kolchinsky, B. D. Tracey, and D. D. Cox. On the information bottleneck theory of deep learning. *Journal of Statistical Mechanics: Theory and Experiment*, 2019(12):124020, 2019.
- [44] Y. Shao, R. D. Cook, and S. Weisberg. Marginal tests with sliced average variance estimation. *Biometrika*, 94(2):285–296, 2007.
- [45] Z. Shen, H. Yang, and S. Zhang. Deep network approximation characterized by number of neurons. *arXiv preprint arXiv:1906.05497*, 2019.
- [46] R. Shwartz-Ziv and N. Tishby. Opening the black box of deep neural networks via information. *arXiv preprint arXiv:1703.00810*, 2017.

- [47] A. Srinivas, M. Laskin, and P. Abbeel. Curl: Contrastive unsupervised representations for reinforcement learning. *arXiv preprint arXiv:2004.04136*, 2020.
- [48] T. Suzuki and M. Sugiyama. Sufficient dimension reduction via squared-loss mutual information estimation. *Neural computation*, 25(3):725–758, 2013.
- [49] G. J. Székely and M. L. Rizzo. Brownian distance covariance. *The annals of applied statistics*, 3(4):1236–1265, 2009.
- [50] G. J. Székely and M. L. Rizzo. The distance correlation t-test of independence in high dimension. *Journal of Multivariate Analysis*, 117:193–213, 2013.
- [51] G. J. Székely, M. L. Rizzo, N. K. Bakirov, et al. Measuring and testing dependence by correlation of distances. *The annals of statistics*, 35(6):2769–2794, 2007.
- [52] N. Tishby and F. Pereira. The information bottleneck method. In *Proceedings of the 37-th Annual Allerton Conference on Communication, Control and Computing*, pages 368–377.
- [53] N. Tishby and N. Zaslavsky. Deep learning and the information bottleneck principle. In *2015 IEEE Information Theory Workshop*, 2015.
- [54] I. Tolstikhin, O. Bousquet, S. Gelly, and B. Schölkopf. Wasserstein auto-encoders. In *ICLR*, 2018.
- [55] M. Tschannen, J. Djolonga, P. K. Rubenstein, S. Gelly, and M. Lucic. On mutual information maximization for representation learning. In *ICLR*, 2020.
- [56] P. Vepakomma, C. Tonde, A. Elgammal, et al. Supervised dimensionality reduction via distance correlation maximization. *Electronic Journal of Statistics*, 12(1):960–984, 2018.
- [57] C. Villani. *Optimal transport: old and new*, volume 338. 2008.
- [58] R. Wang, A.-H. Karimi, and A. Ghodsi. Distance correlation autoencoder. In *IJCNN*, 2018.
- [59] Y. Xia, H. Tong, W. Li, and L.-X. Zhu. An adaptive estimation of dimension reduction space. *Journal of the Royal Statistical Society Series B*, 64(3):363–410, 2002.
- [60] H. Xiao, K. Rasul, and R. Vollgraf. Fashion-mnist: a novel image dataset for benchmarking machine learning algorithms. *arXiv preprint arXiv:1708.07747*, 2017.